

## Crosslinkable micelles from diblock amphiphilic copolymers based on vinylbenzyl thymine and vinylbenzyl triethylammonium chloride

Alejandro L. Barbarini,<sup>1</sup> Diana A. Estenoz,<sup>2</sup> Débora M. Martino<sup>1</sup>

<sup>1</sup>Instituto de Física del Litoral (IFIS Litoral), CONICET - UNL, Güemes 3450, S3000GLN Santa Fe, Argentina

<sup>2</sup>Instituto de Desarrollo Tecnológico para la Industria Química (INTEC) - CONICET - UNL, Güemes 3450, S3000GLN Santa Fe, Argentina

Correspondence to: D. M. Martino (E-mail: debora.martino@santafe-conicet.gov.ar)

**ABSTRACT:** Polymeric micelles (PMs) composed of self-assembled amphiphilic block copolymers were synthesized from vinylbenzyl thymine (VBT) and vinylbenzyl triethylammonium chloride (VBA) exhibiting improved physical stability. Three diblock copolymers of different chemical compositions and similar molecular weights (polydispersities below 1.5) were obtained via nitroxide mediated radical polymerization. Critical micelle concentration (CMC) was determined by dye micellization method, the shift of the absorption peak of the anionic (EY) due to the interactions with non-assembled chains and auto-assembled copolymers was followed. Polymeric systems exhibited good stability revealing that a higher proportion of cationic monomers in the diblock reduce the CMC. Furthermore, after the core of PMs was photocrosslinked by UV irradiation, the CMC decreases notably. Kinetic release studies using EY dye as probe demonstrated that both, higher VBA ratios in the polymer and higher UV-irradiation, slow down the dye release. © 2015 Wiley Periodicals, Inc. *J. Appl. Polym. Sci.* **2015**, *132*, 41947.

**KEYWORDS:** biomimetic; copolymers; drug delivery systems; micelles; stimuli-sensitive polymers

Received 7 July 2014; accepted 2 January 2015

DOI: 10.1002/app.41947

### INTRODUCTION

Nanotechnology has been one of the fastest evolving areas in Science in the past 20 years. The ability to produce and manipulate nanometer-sized structures has solved many technological dilemmas and has opened doors to innovation in multiple fields. In particular, the use of nanoparticles for the development of drug transport devices constitutes an area of current interest.<sup>1–4</sup>

Among the drug transport systems, the nanoscale polymeric micelles (PMs) have triggered greater attention.<sup>5–7</sup> PMs are colloidal particles, typically around 100 nm, composed of amphiphilic block copolymers.<sup>8</sup> The hydrophobic core serves as a reservoir for poorly soluble active species and allows increasing their concentration in hydrophilic solutions.<sup>9</sup> Furthermore, in comparison with surfactant micelles the PMs have a very high thermodynamic stability and, in general, exhibit a Critical Micelle Concentration (CMC) 1000 times lower.<sup>10</sup> Therefore, PMs can be used for solubilization, stabilization, and entrapment of active species<sup>11,12</sup> being one of the most promising ways of controlled release systems.<sup>6,13</sup> However, the application of PMs in industrial reactors is limited due to the dissociation of the micellar core-shell structures. An alternative to improve the physical stability of the PMs is the chemical crosslinking of

the micellar core.<sup>14,15</sup> Riess *et al.*<sup>3</sup> reported an early work of diblock copolymer micelles with crosslinkable hydrophobic groups. Subsequently, several efforts have been made to improve the synthesis of PMs with crosslinkable core or corona, such as synthesizing polymeric segments with functional groups ready to crosslink upon UV irradiation.<sup>16–20</sup>

Controlled radical polymerization (CRPs) enables the production of tailor-made structures of block copolymers and represents an economic alternative to living anionic polymerizations.<sup>21–24</sup> Nitroxide mediated radical polymerization (NMRP) is a CRP based on a dynamic equilibrium between growing free radicals and stable nitroxide radicals.<sup>25–28</sup> The active-dormant interchange minimizes the termination reactions between macroradicals and induces a slow growth of the polymer chains.

Vinylbenzyl thymine (VBT) monomer was designed to have the ability to crosslink upon short wavelength UV light, as a consequence of thymine–thymine cyclobutane ring formation.<sup>29–32</sup> Several copolymers containing VBT have been synthesized by free radical polymerization and crosslinked by UV irradiation.<sup>33–36</sup> In addition, diblock copolymers containing VBT and ionic monomers such as vinylbenzyl sulfonate (VPS) or vinylbenzyl triethylammonium chloride (VBA) have been

synthesized.<sup>37,38</sup> Warner and Saito studied the micelle formation mechanism from self-assembled pVPS-(b)-pVBT copolymers, and their ability to regulate the release of riboflavin.<sup>37</sup> Kaur *et al.* synthesized crosslinkable micelles based on pVBA-(b)-pVBT diblock copolymers obtained by NMRP. The authors reported the significance of hydrogen bonding between neighbor thymines on the micelles formation, and the key role of the core crosslinking on the stability of the formed micelles.<sup>38</sup> However, several features related to the interrelationships between the molecular structure of the copolymers, the micelle formation mechanisms and the ability to control the release processes, still have not being completely elucidated.

In this article, a detailed study of the NMRP copolymerization reaction of VBT and VBA monomers was carried out. Three diblock copolymers of different chemical compositions were synthesized having similar molecular weights, and subsequently used for the formation of micellar systems. The size of the micelles obtained from the diblock copolymers was determined using dynamic light scattering (DLS) and atomic force microscopy (AFM), while the CMC was analyzed by UV-vis spectroscopy. The effects of the length of hydrophilic segments (pVBA) and the crosslinking degree of the micellar core on the CMC were investigated. An in-vitro release study of an anionic dye, eosin Y (EY), was carried out to evaluate the capability to control the dye release as function of the crosslinking degree of the micellar core.

## EXPERIMENTAL

Thymine, triethylamine, 2,2-tetramethylpiperidin-1-oxyl (TEMPO), and EY were purchased from Sigma-Aldrich (Argentina), while vinylbenzyl chloride (VBC), 2,6-di-tertbutyl-4-methylphenol (BHT) and polyethylene glycol/polyethylene oxide standards (Readycal-Kit PEO/PEG) were purchased from Fluka (Argentina), and all used as received. Dimethylformamide (DMF) was purchased from Dorwill (Argentina) and distilled before used. Sodium metabisulfite, potassium persulfate and sodium bromide were purchased from Anedra (Argentina), and sodium hydroxide from Merck (Argentina). Tetrahydrofuran (THF), acetone, ethanol, toluene and ethylene glycol were obtained from Cicarelli (Argentina), while acetonitrile and dimethylsulfoxide (DMSO) from Sintorgan (Argentina). Bidistilled water was used in all reactions. The dialysis Biotech membranes (Cut off = 3500 Da) were purchased from Spectra/Por (USA) and pretreated with bidistilled water as suggested by the manufacturer.

### Synthesis of VBT and Vinylbenzyl Triethylammonium (VBA) Monomers

For the synthesis of VBT monomer the method of Cheng *et al.* was used.<sup>29</sup> Thymine and sodium hydroxide in a 1 : 1 molar ratio were dissolved in a minimum volume of distilled water and the solution was stirred at room temperature for 2 h. Dropping the aqueous solution into ethanol the thymine sodium salt crushed out, and to eliminate any traces of water the thymine sodium salt was lyophilized for 24 h. VBC (45 g – 0.296 mol), lyophilized thymine sodium salt (56.56 g – 0.325 mol), inhibitor BHT (60 mg – 0.25 mmol) and 800 mL of distilled DMF were

added to a three-neck round bottom flask equipped with a condenser, a nitrogen inlet and a magnetic stirrer. The reaction was carried out at 70°C for 24 h under nitrogen atmosphere. The solvent was removed almost completely by rotoevaporation at 35°C and the unreacted thymine was filtrated with boiling toluene. The filtrated solution was cooled at –5°C, and after 24 h, the crystallized VBT was collected by filtration and dried under vacuum (yield = 47%).

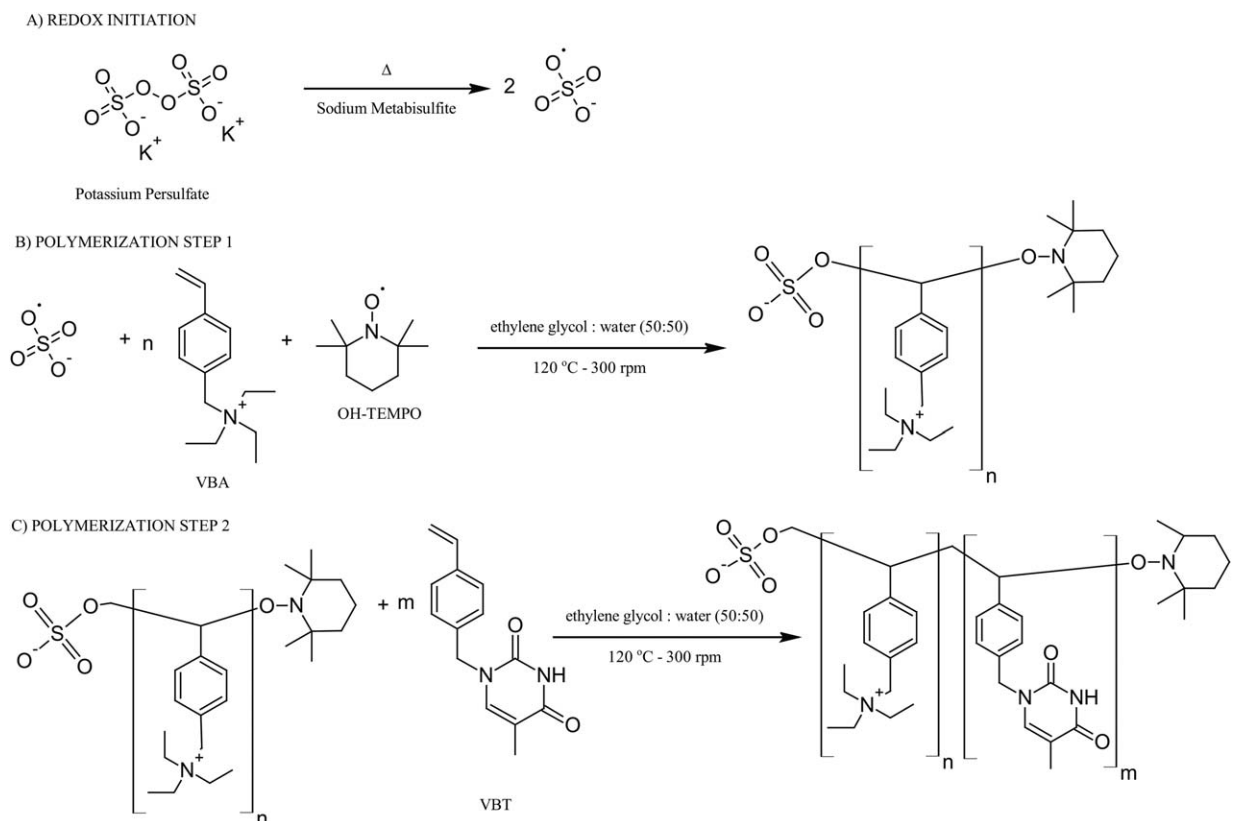
For the VBA synthesis, the method developed by Zarras *et al.* was followed.<sup>39</sup> 50 mL of VBC and 200 mL of acetone were added into a round bottom flask. While the solution was stirring, 50 mL of triethylamine were added, and the reaction was run at 60°C with reflux for 1 h. Then, the heat was turned off and the solution was allowed to stir overnight at room temperature. The precipitated product was filtered and washed with cold acetone (yield = 99%).

### Synthesis of Diblock Copolymer pVBA-(b)-pVBT by Aqueous NMRP

The synthesis of diblock copolymers was performed following the procedure described by Kaur *et al.*<sup>38</sup> The reaction was carried out in two steps: in the first step, pVBA was polymerized using a redox initiation system, and in the second step the diblock copolymer was obtained by polymerization of VBT from the pVBA macroinitiator formed in the first step. A general method is presented in Scheme 1.

Initially VBA and TEMPO (0.0115 g – 0.0736 mmol) were dissolved in 10 mL of ethylene glycol : water (50 : 50) mixture. The redox initiators, sodium metabisulfite ( $\text{Na}_2\text{S}_2\text{O}_5$ ) (0.01 g – 0.06 mmol) and potassium persulfate ( $\text{K}_2\text{S}_2\text{O}_8$ ) (0.012 g – 0.04 mmol), were dissolved separately in the same solvent mixture. The solution containing the initiator was injected into the reaction system and oxygen was removed by nitrogen bubbling for 15 min. Then, the temperature was increased to 125°C under stirring and nitrogen atmosphere. The synthesis took place under these conditions for 24 h. Samples were taken at different times along the reaction, to determine the conversion ( $x$ ) by gravimetry, and the average molecular weights by size exclusion chromatography (SEC). The synthesis was stopped by cooling it in ice bath. The final products and each sample taken along the reaction were precipitated by slowly adding the solution into cold acetone under vigorous stirring and then dried under vacuum.

In the second step, the macroinitiators pVBA-TEMPO, the VBT monomer and 15 mL of ethylene glycol : water (50 : 50) mixture were added into a three-neck flask. Nitrogen was bubbled into the solution for 15 min while stirring. The temperature was increased to 125°C keeping the nitrogen atmosphere, and the synthesis was carried out under these conditions for 24 h. The conversion and the average molecular weights were also measured along the reaction as explained before. Following this procedure, pVBA-(b)-pVBT diblock copolymers with different chemical compositions in the range of 20–80% VBT were synthesized, having approximately the same molecular weights. The reactions were carried out by duplicate, and the mean values are shown. Table I shows the experimental composition for each polymerization reaction.



**Scheme 1.** Synthesis of diblock copolymers pVBA-(b)-pVBT by aqueous NMRP. (A) Redox initiation system, (B) Polymerization-Step 1: synthesis of pVBA and, (C) Polymerization-Step 2: synthesis of pVBT from pVBA macroinitiator.

### Copolymers Characterization

The final products of each reaction step and the samples taken along the reactions were characterized by gravimetry as follows. Each polymer was precipitated in 100 mL of cold acetone and dried under vacuum at 65°C until constant weight. Molecular weight determinations were carried out using a SEC instrument equipped with an injector Waters 717 plus Autosampler and a refractive index detector Waters 2414. For the pVBA samples, a set of five columns Ultrahydrogel WATERS (7.8–300 mm) were used. The carrier solvent was water : acetonitrile (80 : 20) with NaBr (0.5M) at 0.8 mL.min<sup>-1</sup> and 25°C. For the diblock copolymer, a set of 7 columns Styragel (7.8–300 mm) was used and the carrier was THF at 1 mL.min<sup>-1</sup> and 25°C.

### Micelle Formation

Self-assembly of diblock copolymers was induced by dialysis with buffer substitution. A 1% copolymer solution in DMSO was filtered through a 0.45 μm syringe filter (Microclar) and

added into a dialysis tubular membrane (Spectra/Por - Cut off = 3500 Da). Dialysis was carried out using a volume of external bidistilled water 10 times larger than the DMSO volume. The total dialysis time was 42 h, and the external volume was replaced with fresh bidistilled water following three cycles: every 1, 5, and 8 h.

### Determination of CMC

The CMC was determined by the dye micellization method, which detects the presence of micelles in the solution.<sup>40</sup> The shift of the characteristic visible absorption spectra of EY dye as a consequence of its interactions with non-assembled chains and auto-assembled copolymers was followed. The copolymer micelles were made up by dialysis as described before. Subsequently, different dilutions covering a broad range of concentrations were prepared and 10 μL of aqueous EY (9 mM) were added to each dilution. UV-Vis spectra were taken using a Lambda 20 Perkin Elmer UV/Vis Spectrophotometer. The shift

**Table I.** Experimental Composition for Each Polymerization Reaction: DB1, DB2, and DB3

	Diblock 1 (DB1)		Diblock 2 (DB2)		Diblock 3 (DB3)	
	Mol (mmol)	Molar Ratio <sup>a</sup>	Mol (mmol)	Molar Ratio <sup>a</sup>	Mol (mmol)	Molar ratio <sup>a</sup>
VBA	4.12	89.83	6.19	134.97	4.12	89.83
VBT	3.74	81.46	3.74	81.46	6.18	134.71

<sup>a</sup> Monomer/potassium persulfate molar ratio.

**Table II.** Number-Average Molecular Weight ( $M_n$ ), Weight-Average Molecular Weight ( $M_w$ ), Polydispersity ( $I_p = M_w/M_n$ ), and Conversion ( $x$ ) of pVBA Macroinitiators and Final Diblock Copolymers

Reaction	pVBA				pVBA-(b)-pVBT				VBT:VBA Molar Ratio
	$M_n$	$M_w$	$I_p$	$x$	$M_n$	$M_w$	$I_p$	$x$	
DB1	8300	10,600	1.3	0.42	13,900	18,800	1.3	0.46	40:60
DB2	14,300	18,300	1.3	0.87	17,400	22,600	1.3	0.44	18:82
DB3	3500	4100	1.2	0.34	14,700	18,100	1.2	0.66	76:24

VBT:VBA molar ratio indicates the contribution of each segment to the final diblock copolymer.

of the absorbance peak from  $\lambda = 518$  nm in water to  $\lambda = 530$  nm in micellar environment was followed, and the CMC was established. The same procedure was used for the synthesized pVBA-(b)-pVBT copolymers.

### Particle Size Measurements

The particle size distribution of the self-assembled micellar system was determined by DLS (Brook-Haven BI-2030 Dynamic Light Scattering Photometer) at 25°C, a detection angle of 90° and irradiation wavelength  $\lambda = 630$  nm. Considering that the dynamic of these systems can be complex, to find the diffusion coefficients and the particle size distributions, a multiple exponential function was used to analyze the intensity correlation functions.

Atomic Force Microscopy (AFM) images were acquired with a commercial Nanotec Electronic System (Nanotec Electrónica S.L., Madrid, Spain) operating in tapping mode at atmosphere pressure and room temperature. Acquisition and image processing were performed using the WS×M free software.<sup>41</sup> V-shaped Olympus RC800PSA cantilevers (Olympus Corporation, Tokyo, Japan) made of silicon nitride coated with Au/Cr on the back side to enhance reflectivity were used, having a resonance frequency in the range of 70–90 kHz, nominal spring constant between 0.05 and 0.1 N.m<sup>-1</sup> and radius smaller than 20 nm. The samples were prepared spreading the micellar solution onto a clean glass slide and subsequently drying them in a vacuum oven at 60°C for 30 min.

### Micelle Core Crosslinking

To enhance the stability of the micellar system the pVBT segments forming the micelle core were crosslinked using UV light. Following the described procedure, micelles were prepared by dialysis from highly concentrated copolymer solutions, and then irradiated with UV light at various irradiation doses between 0 J cm<sup>-2</sup> and 10 J cm<sup>-2</sup> ( $\lambda = 254$  nm – CL 1000 Ultraviolet Crosslinker). Subsequently, different dilutions of irradiated micelles containing 10  $\mu$ L of aqueous EY (9 mM) were prepared. The corresponding UV-vis spectra were taken after each irradiation.

### Kinetics of EY Release

The EY dye was used as probe to study the release kinetics. Aqueous pVBA-(b)-pVBT micelle solutions with concentrations above the CMC were prepared with the same initial EY concentration (24 mM) and dialyzed for 3 h against bidistilled water (five times the volume of micelle used), using a dialysis membrane with cut off = 3500 Da. Samples from the external

medium were taken at different times, and replaced by the same volume of fresh bidistilled water after each sampling. The UV-vis spectra of each sample were recorded and the maximum absorption peak of EY in aqueous environment was followed. The release profiles of EY in both micelles (DB1 and DB2) were compared with the release kinetics of EY in aqueous solution at the same concentration (24 mM). In addition, the effect of the micelles crosslinking degree on the EY release was evaluated in function of the UV irradiation dose.

## RESULTS AND DISCUSSION

### Characterization of pVBA-(b)-pVBT diblock copolymers

Table II presents the results of the molecular weight characterization corresponding to the pVBA macroinitiators and the diblock copolymers. The monomer ratios in the block copolymers of Table II estimated from the average molecular weights approximately match the monomer ratios predicted from the monomer feed ratios, and the conversion in each step. Note that the level of conversion reached in each step was not 100%

However, the control of the NMRP reaction was evaluated following the polymerization rate, and the evolution of molecular weights and polydispersity as function of conversion ( $x$ ). Another feature indicating a good radical process control is the linear evolution of the natural logarithm of the initial and instantaneous concentration of monomers ratio [ $\ln([M_0]/[M])$ ] along the reaction time.<sup>42,43</sup> Figure 1 shows the evolution of ( $\ln([M_0]/[M])$ ) as function of time and the polydispersity with the conversion, for the first and second step of the DB1 polymerization reaction. Even though for step 1 the achieved conversion was lower than 100%, the remaining VBA monomer was removed before the beginning of step 2. The absence of VBA was guaranteed by SEC measurements.

The evolution of  $\ln([M_0]/[M])$  as function of time during the first and second steps [Figures 1(A,B)] are both linear. Also, the polydispersity ( $I_p$ ) was kept below 1.5 during the reaction indicating a good control of the polymerization. Similar results for the evolution of  $M_n$  and  $I_p$  (not shown) were obtained for the copolymerization reactions carried out with different copolymer ratios, DB2 and DB3.

### Micelle Formation and Analysis of Particle Size

Scheme 2 shows an illustration of the entire micelle formation process and the subsequent crosslink. First the di-block copolymer is completely dissolved in DMSO [Scheme 2(A)]. Then, the buffer exchange is carried out by dialysis [Scheme 2(B)] and the

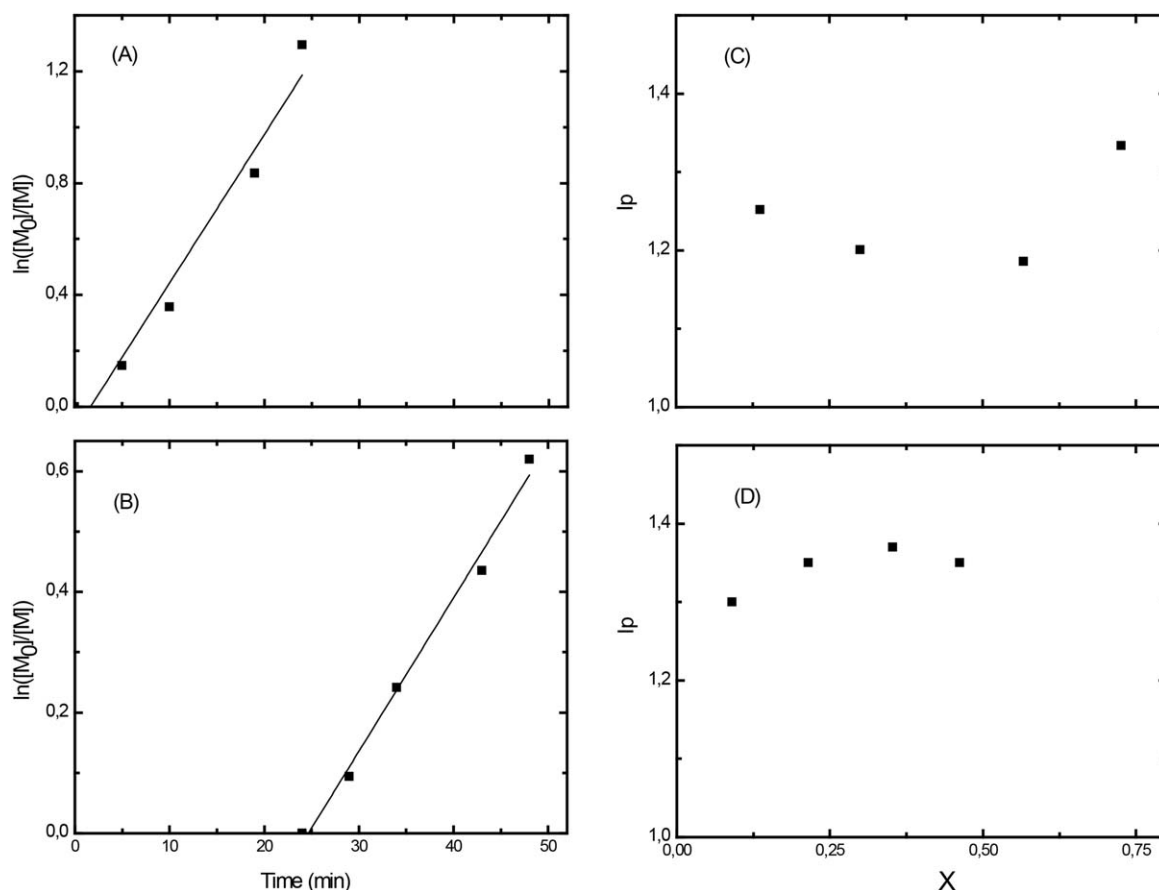


**Figure 1.** DB1 synthesis.  $\ln([M_0]/[M])$  as a function of time and polydispersity ( $I_p$ ) as function of conversion for step 1 (A and C) and step 2 (B and D), respectively.

DMSO is replaced by aqueous buffer. Due to the low affinity of the pVBT segments for the aqueous, and the high solubility of pVBA segments, the di-block tend to self-assemble into micelles. Finally, crosslinking of the micelles core is achieved by UV irradiation of the aqueous suspension [Scheme 2(C)].

Formation of micellar nanoparticles was carried out for the three diblock copolymers synthesized following the procedure described in the “Experimental” Section. After the dialysis process, solutions of copolymers DB1 and DB2 showed an opalescent aspect, typical of Rayleigh scattering, due to formation of micelles.<sup>44</sup> In contrast, the solution of copolymer DB3 showed a transparent appearance indicating the absence of self-assembled micelles at the concentration level tested, and consequently this composition was not employed in following studies. The lack of micelles can be attributable to the presence of a small cationic segment (pVBA) in DB3, since is known that the self-assembling capacity of charged copolymers to form micelles improves when the charge of the molecule increases.<sup>45,46</sup>

DLS measurements were performed on DB1 and DB2 non-irradiated micelles ( $0 \text{ J}\cdot\text{cm}^{-2}$ ). The average diameter ( $d_a$ ) of the micelles and the corresponding standard deviations ( $\sigma$ ) resulting from the fitting with multiple exponentials model are summarized in the second and fifth columns of Table III. It was observed that DB2 copolymer micelles have a smaller average

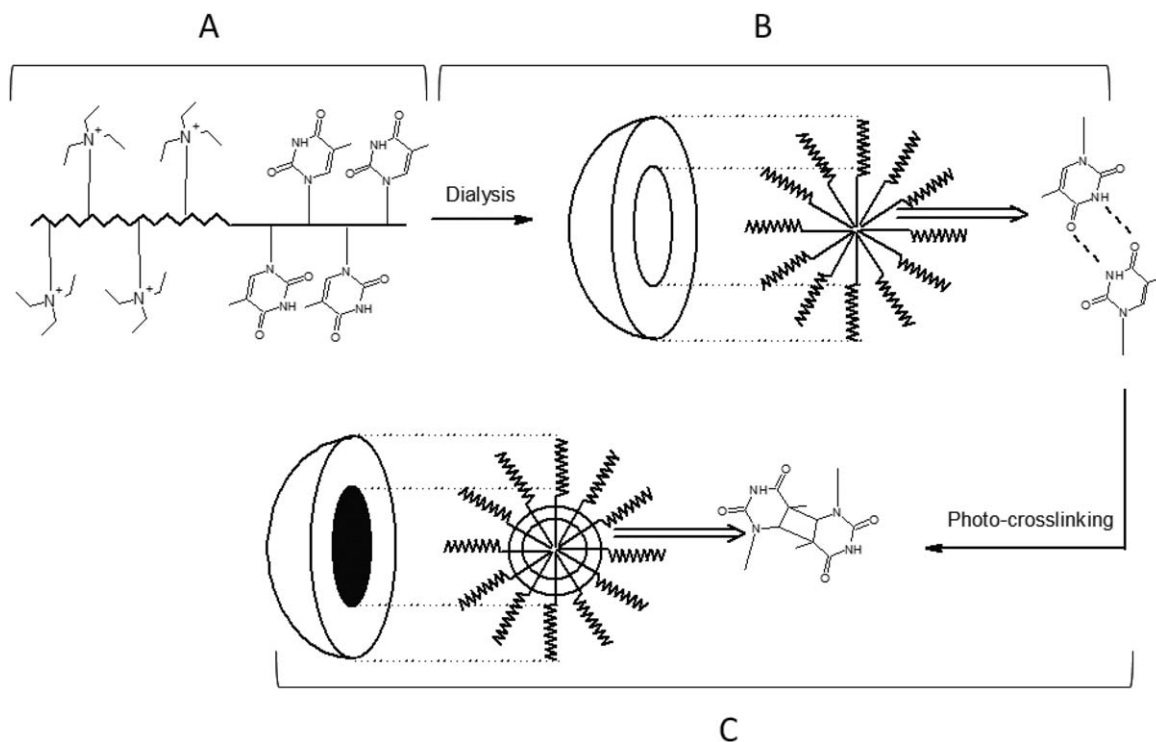
size and a narrower size distribution than DB1 micelles. The smaller size of DB2 micelles is associated to a shorter chain length, and consequently a reduced hydrodynamic volume, of the hydrophobic block forming the micelle core of DB2. The narrower size distribution of DB2 could be associated to the polydispersity of that block. AFM measurements were also carried out for both micelles solutions to validate DLS results, and the micrograph for DB1 micelles is shown in Figure 2. A good agreement between the diameters obtained with both techniques was observed. AFM images also confirmed the lack of micelle-aggregates.

In addition, the effect of the photoinduced thymine dimerization on the particle size distribution was studied. DB1 and DB2 micelle solutions were irradiated with UV light ( $\lambda = 245 \text{ nm}$ ) at  $2 \text{ J}\cdot\text{cm}^{-2}$  and  $5 \text{ J}\cdot\text{cm}^{-2}$  producing a decrease of the average particle size ( $d_a$ ) up to 25% for DB1 and 5% for DB2, caused by the crosslinking of the micelles core (Table III). Also, it can be noted that the particle size distribution gets significantly narrower upon irradiation for both micellar systems.

#### Determination of CMC

For colloidal chemistry, CMC is defined as the amphiphilic macromolecule concentration above which self-assembled micelles are formed.<sup>47</sup> By means of the dye micellization method, the CMC was determined following the shift of the





**Scheme 2.** Micelle formation and subsequent crosslinking processes. (A) Block copolymer dissolved in DMSO, (B) Dialysis and self-assembled micelles formation, (C) UV irradiation of the aqueous suspension.

visible absorption spectra of EY dye. The aqueous solution of EY exhibits an intense band at 518 nm corresponding to the monomeric form of EY, with a shoulder at 496 nm due to the dimeric form of the dye (spectra not shown). It is known that in aqueous solution xanthene dyes have strong interactions with oppositely charged polyelectrolytes, mainly electrostatics.<sup>48,49</sup> Small changes on the dye peak positions suggest changes on the polarity of the surrounding matrix, and on the degree of compartmentalization of the micro-heterogeneous system.<sup>50</sup>

For each micellar system DB1 and DB2, a series of dilutions were prepared adding the same amount of EY dye (9 mM), and the variations on the spectral behavior of EY in the presence of micelles were studied. Figure 3(A) shows the changes observed on the absorption spectra of EY as function of wavelength, for different DB1 micelle concentrations ranging from  $C_M = 0.007 \text{ mg.mL}^{-1}$  to  $C_M = 1 \text{ mg.mL}^{-1}$ . The maximum absorption peak of EY in water shifted to higher wavelengths (from 518 to 530 nm in the  $C_M$  range studied) upon the progressive addition of cationic diblock pVBA-(b)-pVBT copolymers. Such spectral shift in the presence of micelles is common,

indicating electrostatic interactions between EY and the oppositely charged pVBA segments of the micelles. The red shift of the spectra assigned to the monomeric dye is an evidence of the polarity change in both environments.

From Figure 3(A), besides the red shift it can be observed that the intensity of the maximum absorption peak of EY decreases with the addition of diblock copolymers until a certain concentration, and subsequently starts to grow. Figure 3(B) depicts the

**Table III.** Average Diameter ( $d_a$ ) of Micelles and Corresponding Standard Deviations ( $\sigma$ ) From DLS Measurements

Irradiation dose ( $\text{J.cm}^{-2}$ )	DB1 micelles			DB2 micelles		
	0	2	5	0	2	5
$d_a$ (nm)	190	150	140	125	120	120
$\sigma$	100	40	20	30	20	20

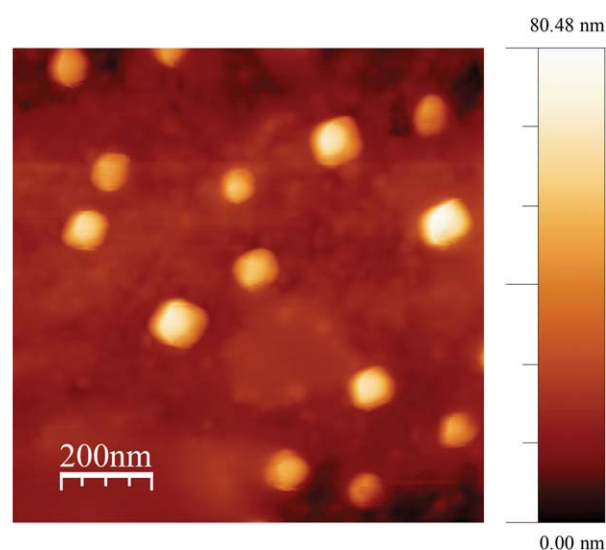


**Figure 2.** AFM micrograph of DB1 micelles formed by self-assembly of diblock copolymers. [Color figure can be viewed in the online issue, which is available at wileyonlinelibrary.com.]

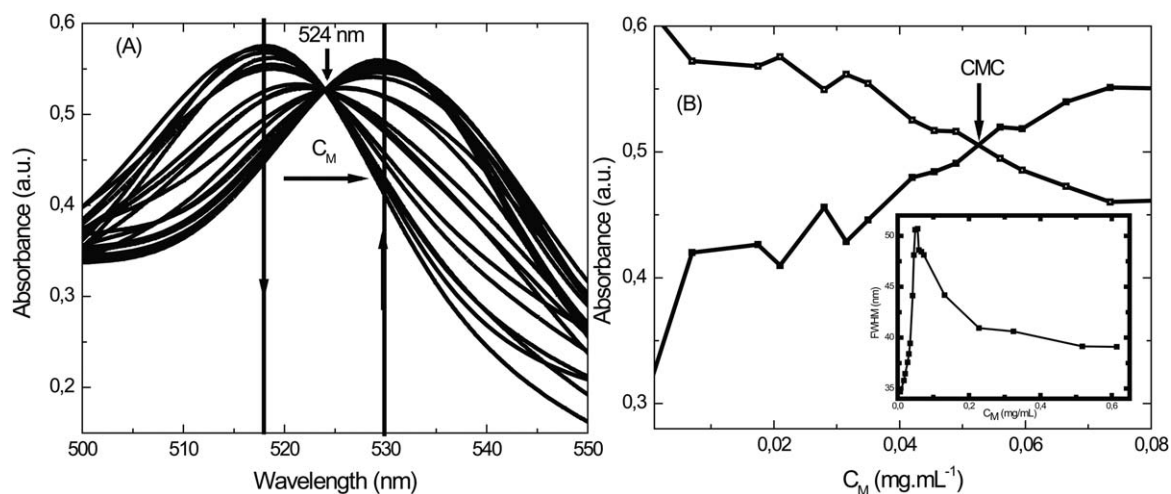


**Figure 3.** (A) Dye absorption spectra in function of wavelength for DB1 micelles at different concentrations ( $C_M$  between  $0.007 \text{ mg mL}^{-1}$  to  $1 \text{ mg mL}^{-1}$ ) and  $[EY] = 9 \text{ mM}$ ; (B) Evolution of the dye absorbance ( $[EY] = 9 \text{ mM}$ ) against DB1 micelle concentration ( $C_M$ )  $\square$  518 nm and  $\blacksquare$  530 nm. Inset: FWHM of the spectra in function of micelle concentration ( $C_M$ ).

evolution of the maximum absorption peaks at 518 and 530 nm, as function of DB1 diblock copolymer concentration ( $C_M$ ). Two different phases for the spectroscopic properties of the dye in function of the DB1 micelle concentration are clearly shown. Approximately up to  $0.05 \text{ mg mL}^{-1}$ , the increase of  $C_M$  produces a noticeable reduction of the maximum absorption peak at 518 nm. Simultaneously, with the addition of small quantities of diblock copolymer the broadening of the absorption band calculated as the full width at half maximum (FWHM) enhances abruptly, reaching a maximum around  $0.055 \text{ mg mL}^{-1}$  [see inset in Figure 3(B)]. These spectral changes are governed by the electrostatic attraction between the anionic dye and the cationic diblock pVBA-(b)-pVBT copolymer. In the  $C_M$  range studied, an isosbestic point was observed at 524 nm indicating that the spectral changes are connected to the existence of two types of “association sites” between the dye and the diblock pVBA-(b)-pVBT copolymers, both single chains and self-assembled copolymers. For higher micelle concentrations a significant increase of the EY absorption peak at 530 nm was observed, accompanied with a decrease of the bandwidth FWHM until recovering practically the initial value [inset in Figure 3(B)]. Those changes indicate the formation of a region that provides the monomeric dye a microenvironment less polar than water.

CMC was estimated from the intersection point of both curves displayed in Figure 3(B). The resulting CMC value was  $0.053 \text{ mg mL}^{-1}$  for DB1 system, in good agreement with previously reported CMC values for similar copolymer systems obtained by other techniques.<sup>38</sup>

Figure 4 compares the evolution of the absorption peaks of EY at 518 nm and 530 nm as function of diblock copolymer concentration for DB1 and DB2 micellar solutions without irradiation. Results for DB2 diblock copolymers show an earlier intersection point compared to DB1 diblock copolymers ( $\text{CMC} = 0.012 \text{ mg mL}^{-1}$ ) that can be attributed to the presence of higher proportion of charged VBA monomer in the structure of DB2. High dilution medium is necessary to overcome the

electrostatic repulsions between charged groups during the aggregation process. It is well known that for amphiphilic macromolecules with ionic charge, the tendency to form micellar structures is enhanced when the ionic charge on the hydrophilic segment increases.<sup>45,46</sup>

The effect of the crosslinking of the micellar core on the CMC value was investigated. Figure 5 compares the evolution of the absorption peaks at 518 nm and 530 nm as function of diblock copolymer concentration for DB1 copolymers irradiated with UV light between 0 and  $5 \text{ J cm}^{-2}$ . The CMC decreases from  $0.053 \text{ mg mL}^{-1}$  in absence of irradiation ( $0 \text{ J cm}^{-2}$ ) to  $0.024 \text{ mg mL}^{-1}$  at  $2 \text{ J cm}^{-2}$  and to  $0.013 \text{ mg mL}^{-1}$  at  $5 \text{ J cm}^{-2}$ . This behavior is a consequence of the dimerization reactions taking place between adjacent thymines in the core of the micelle that stabilizes the micellar system even for extreme dilutions. These results provide a technological advantage over other

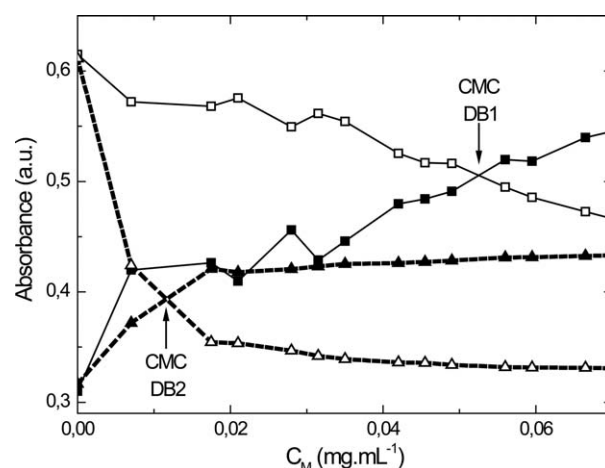


**Figure 4.** Evolution of the dye absorbance as function of copolymer concentration for DB1 ( $\square$  518 nm,  $\blacksquare$  530 nm) and DB2 ( $\Delta$  518 nm,  $\blacktriangle$  530 nm) micelles.

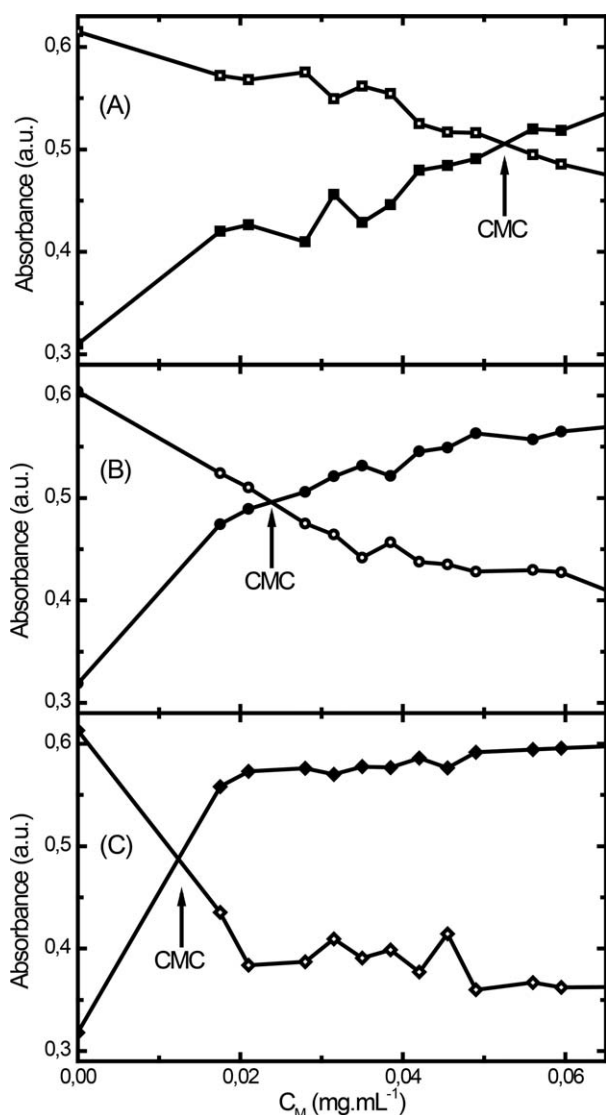


**Figure 5.** Evolution of the absorption peaks at 518 nm and 530 nm as function of copolymer concentration for DB1 micelles using different irradiation doses: (A)  $0 \text{ J cm}^{-2}$  ( $\square$  518 nm,  $\blacksquare$  530 nm), (B)  $2 \text{ J cm}^{-2}$  ( $\circ$  518 nm,  $\bullet$  530 nm) and (C)  $5 \text{ J cm}^{-2}$  ( $\diamond$  518 nm,  $\blacklozenge$  530 nm).

systems, in view of the fact that crosslinkable micellar systems can be used below their CMC if they are previously irradiated with a selective dose of UV light.

#### Controlled Release Kinetics

For the technological applications of these micellar systems, it is important to establish the effect of copolymer composition and curing conditions on the release kinetics. Two aqueous solutions of DB1 and DB2 micelles with concentrations slightly above the CMC ( $0.059 \text{ mg.mL}^{-1}$  and  $0.018 \text{ mg.mL}^{-1}$ , respectively), and 24 mM of EY were prepared and dialyzed as described in the Experimental Section. Samples were taken from the external volume at 15, 30, 45, 60, 120, and 180 min, and replaced with fresh bidistilled water. As a comparison, an aqueous solution of EY (24 mM) was dialyzed and samples were taken using the same procedure. The UV-vis spectra of each sample were

recorded and the evolution of the EY absorption peak at 524 nm (corresponding to the maximum absorption at the CMC value) was followed and presented in Figure 6. In particular, Figure 6(A) clearly shows that for both systems there is a control of the EY release. Also, it is observed that DB2 micelles exhibit a slower release rate due to the higher amount of positive charged groups that interact with ionic EY dye.

Micellar solutions of DB1 and DB2 copolymers were irradiated with UV light at  $1 \text{ J.cm}^{-2}$  and  $5 \text{ J.cm}^{-2}$  to evaluate the influence of the crosslinking degree on the kinetics release of EY dye (24 mM). Figure 6(B,C) show that the photoinduced crosslinking of thymine moieties in the core of the micelles slows down the release rate of EY in both copolymer micelles. In addition, the maximum EY release decreases from 0.59 to 0.39 mM for DB1, and 0.42 to 0.21 mM for DB2.

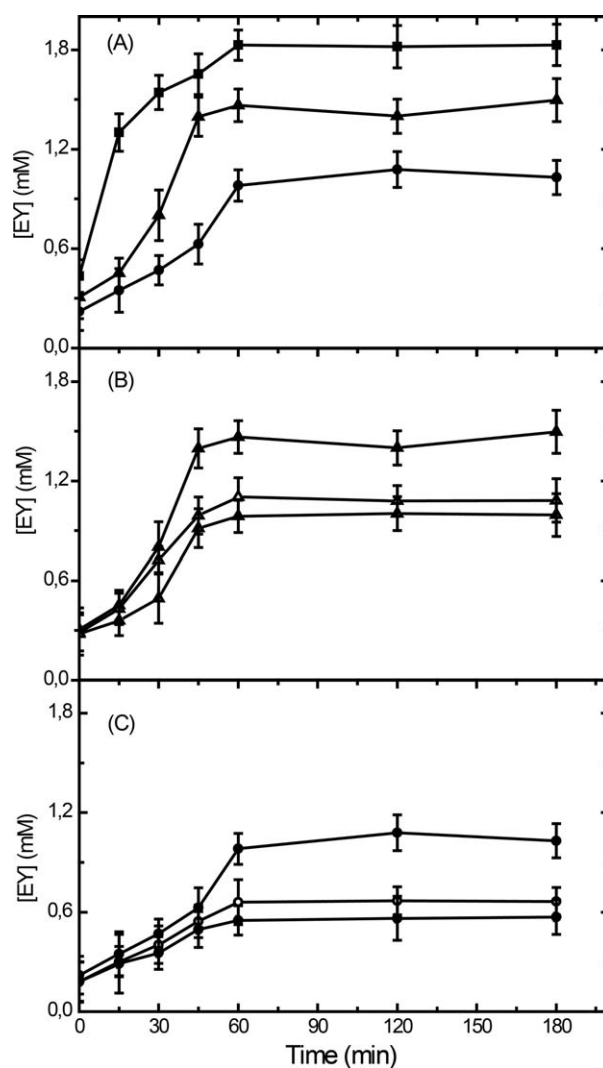


**Figure 6.** Evolution of EY maximum absorption peak at  $\lambda = 524 \text{ nm}$  as function of time for: (A)  $\blacksquare$  aqueous solution,  $\blacktriangle$  DB1 and  $\bullet$  DB2 micelles without irradiation, (B) DB1 irradiated micelles ( $\blacktriangle$   $0 \text{ J cm}^{-2}$ ,  $\triangle$   $1 \text{ J cm}^{-2}$ ,  $\bullet$   $5 \text{ J cm}^{-2}$ ) and (C) DB2 irradiated micelles ( $\bullet$   $0 \text{ J cm}^{-2}$ ,  $\circ$   $1 \text{ J cm}^{-2}$ ,  $\blacktriangle$   $5 \text{ J cm}^{-2}$ ).



## CONCLUSIONS

Three pVBA-(b)-pVBT diblock copolymers of similar molecular weight but different molar ratios were obtained by NMRP. The characterization of the SEC results showed a good reaction control and low polydispersities. Diblock copolymers with VBA molar fraction higher than at least 50% were able to form micelles exhibiting elevated self-assemble capacity due to the presence of charged groups. DLS and AFM characterization indicated a nanometric size distribution of self-assembled micelles, and the absence of aggregates. In addition, it was observed that the particle size can be controlled by the photoinduced crosslinking of the core using UV light. The tendency to form micellar structures was enhanced when the ionic charge on the hydrophilic segment was augmented, as well as with the photoinduced crosslinking of the micelles core. The analysis of the EY spectral changes detected in the presence of diblock copolymer suggested that the EY dye is sensing two different media depending on the environment. The release kinetics for both micellar systems was controlled exhibiting a slower release rate when higher amount of positive charged groups were present. Furthermore, it was possible to modify the release kinetics by irradiating and crosslinking of the micelles core. The obtained results can be used for innovative technological applications. Forthcoming works plan to evaluate the ability of the micellar systems to control the release of other molecules, and to explore the mechanisms that govern the release kinetics.

## ACKNOWLEDGMENTS

DMM and DAE are members of the Research Council of CONICET. Authors would like to thank Universidad Nacional del Litoral, CONICET, and MinCyT of Argentina for the financial support.

## REFERENCES

1. Rapoport, N. *Prog. Polym. Sci.* **2007**, *32*, 962.
2. Harada, A.; Kataoka, K. *Prog. Polym. Sci.* **2006**, *31*, 949.
3. Riess, G. *Prog. Polym. Sci.* **2003**, *28*, 1107.
4. Gil, E. S.; Hudson, S. M. *Prog. Polym. Sci.* **2004**, *29*, 1173.
5. Jackson, J. K.; Hung, T.; Letchford, K.; Burt, H. M. *Int. J. Pharm.* **2007**, *342*, 6.
6. Kataoka, K.; Harada, A.; Nagasaki, Y. *Adv. Drug Delivery Rev.* **2012**, *64*, 37.
7. Kuskov, A. N.; Shtilman, M. I.; Goryachaya, A. V.; Tashmuhamedov, R. I.; Yaroslavov, A. A.; Torchilin, V. P.; Tsatsakis, A. M.; Rizos, A. K. *J. Non-Cryst. Solids* **2012**, *353*, 3969.
8. Kim, S. Y.; Shin, I. G.; Lee, Y. M. *J. Control. Release* **1998**, *56*, 197.
9. Croy, S. R.; Kwon, G. S. *Curr. Pharm. Des.* **2006**, *12*, 4669.
10. Yamamoto, Y.; Yasugi, K.; Harada, A.; Nagasaki, Y.; Kataoka, K. *J. Control. Release* **2002**, *82*, 359.
11. Yao, J.; Ju, R. J.; Wang, X. X.; Zhang, Y.; Li, R. J.; Yu, Y.; Zhang, L.; Lu, W. L. *Biomaterials* **2011**, *32*, 3285.
12. Benny, O.; Fainaru, O.; Adini, A.; Cassiola, F.; Bazinet, L.; Adini, I.; Pravda, E.; Nahmias, Y.; Koirala, S.; Corfas, G.; D'Amato, R. J.; Folkman, J. *Nat. Biotechnol.* **2008**, *26*, 799.
13. Kataoka, K.; Kwon, G. S.; Yokoyama, M.; Okano, T.; Sakurai, Y. *J. Control. Release* **1993**, *24*, 119.
14. Kakizawa, Y.; Harada, A.; Kataoka, K. *J. Am. Chem. Soc.* **1999**, *121*, 11247.
15. Shuai, X.; Merdan, T.; Schaper, A. K.; Xi, F.; Kissel, T. *Bioconjugate Chem.* **2004**, *15*, 441.
16. Thurmond, K. B.; Huang, H.; Clark, C. G.; Kowalewski, T.; Wooley, K. L. *Colloids Surf. B* **1999**, *16*, 45.
17. Jamroz-Piegza, M.; Wałach, W.; Dworak, A.; Trzebicka, B. *J. Colloid Interface Sci.* **2008**, *325*, 141.
18. Wu, Y.; Chen, W.; Meng, F.; Wang, Z.; Cheng, R.; Deng, C.; Liu, H.; Zhong, Z. *J. Control. Release* **2012**, *164*, 338.
19. Zhang, J.; Gong, M.; Yang, S.; Gong, Y. *J. Control. Release* **2011**, *152*, e23.
20. Lu, Y.; Ballauff, M. *Prog. Polym. Sci.* **2011**, *36*, 767.
21. Rösler, A.; Vandermeulen, G. W. M.; Klok, H. *Adv. Drug Delivery Rev.* **2012**, *64*, 270.
22. Goto, A.; Fukuda, T. *Prog. Polym. Sci.* **2004**, *29*, 329.
23. Fischer, H. *Chem. Rev.* **2001**, *101*, 3581.
24. Tang, W.; Tsarevsky, N. V.; Matyjaszewski, K. *J. Am. Chem. Soc.* **2006**, *128*, 1598.
25. Tang, W.; Fukuda, T.; Matyjaszewski, K. *Macromolecules* **2006**, *39*, 4332.
26. Hawker, C. J.; Bosman, A. W.; Harth, E. *Chem. Rev.* **2001**, *101*, 3661.
27. Benoit, D.; Grimaldi, S.; Robin, S.; Finet, J.-P.; Tordo, P.; Gnanou, Y. *J. Am. Chem. Soc.* **2000**, *122*, 5929.
28. Nicolas, J.; Ruzette, A.-V.; Farcet, C.; Gérard, P.; Magnet, S.; Charleux, B. *Polymer* **2007**, *48*, 7029.
29. Cheng, C. M.; Egbe, M. I.; Grasshoff, J. M.; Guarrera, D. J.; Pai, R. P.; Warner, J. C.; Taylor, L. D. *J. Polym. Sci., Part A: Polym. Chem.* **1995**, *33*, 2515.
30. Grasshoff, J. M.; Taylor, L. D.; Warner, J. C. Vinylbenzyl thymine monomers. U.S. Patent 5,455,349, October 3, 1995.
31. Lamola, A. A.; Mittal, J. P. *Science* **1966**, *154*, 1560.
32. Harm, W. In *Biological Effects of Ultraviolet Radiation*; Cambridge University Press: Cambridge, **1980**.
33. Dahman, Y.; Puskas, J. E.; Margaritis, A.; Merali, Z.; Cunningham, M. *Macromolecules* **2003**, *36*, 2198.
34. Bianchini, J. R.; Saito, K.; Balin, T. B.; Dua, V.; Warner, J. C. *J. Polym. Sci., Part A: Polym. Chem.* **2007**, *45*, 1296.
35. Barbarini, A. L.; Estenoz, D. A.; Martino, D. M. *Macromol. React. Eng.* **2010**, *4*, 453.
36. Bortolato, S. A.; Thomas, K. E.; McDonough, K.; Gurney, R. W.; Martino, D. M. *Polymer* **2012**, *53*, 5285.
37. Warner, J. C.; Saito, K. *Green Chem. Lett. Rev.* **2009**, *2*, 71.
38. Kaur, G.; Chang, S. L. Y.; Bell, T. D. M.; Hearn, M. T. W.; Saito, K. *J. Polym. Sci., Part A: Polym. Chem.* **2011**, *49*, 4121.
39. Zarras, P.; Vogl, O. *J. Macromol. Sci., Part A: Pure Appl. Chem.* **2000**, *37*, 817.

40. Suradkar, Y. R.; Bhagwat, S. S. *J. Chem. Eng. Data* **2006**, *51*, 2026.
41. Horcas, I.; Fernández, R.; Gómez-Rodríguez, J. M.; Colchero, J.; Gómez-Herrero, J.; Baro, A. M. *Rev. Sci. Instrum.* **2007**, *78*, 013705.
42. Guillaneuf, Y.; Gigmes, D.; Marque, S. R. A.; Tordo, P.; Bertin, D. *Macromol. Chem. Phys.* **2006**, *207*, 1278.
43. Studer, A.; Schulte, T. *Chem. Rec.* **2005**, *5*, 27.
44. Bespalov, V. I.; Kubarev, A. M.; Pasmanik, G. A. *Radiophys. Quantum Electron.* **1973**, *13*, 1103.
45. Gao, Z.; Varshney, S. K.; Wong, S.; Eisenberg, A. *Macromolecules* **1994**, *27*, 7923.
46. Zhang, L.; Khougaz, K.; Moffitt, M.; Eisenberg, A. In *Amphiphilic Block Copolymers: Self Assembly and Applications*; Elsevier: Amsterdam, **2000**, p 87.
47. McNaught, A. D.; Wilkinson, A. In *IUPAC Compendium of Chemical Terminology ("Gold Book")*, 2nd ed.; Nic, M.; Jirat, J.; Kosata, B.; Jenkins A. D. 2006. Blackwell Scientific Publications: Oxford, UK, **1997**. Available at: <http://gold-book.iupac.org>, accessed June 25, 2014.
48. Mirenda, M.; Dicalio, L. E.; San Roman, E. *J. Phys. Chem. B* **2008**, *112*, 12201.
49. Birla, L.; Cristian, A. M.; Hillebrand, M. *Spectrochim. Acta, Part A* **2004**, *60*, 551.